

Identification of prognostic genes and construction of a novel gene signature in the skin melanoma based on the tumor microenvironment

Wang Yingjuan, MD^{ID}, Zhang Li, MD, Cao Wei, MD, Wang Xiaoyuan, MD*

Abstract

Skin melanoma remains a highly prevalent and yet deadly form of cancer, with the exact degree of melanoma-associated mortality being strongly dependent upon the local tumor microenvironment. The exact composition of stromal and immune cells within this microenvironmental region has the potential to profoundly impact melanoma progression and prognosis. As such, the present study was designed with the goal of clarifying the predictive relevance of stromal and immune cell-related genes in melanoma patients through comprehensive bioinformatics analyses. We therefore analyzed melanoma sample gene expression within The Cancer Genome Atlas database and employed the ESTIMATE algorithm as a means of calculating both stromal and immune scores that were in turn used for identifying differentially expressed genes (DEGs). Subsequently, univariate analyses were used to detect DEGs associated with melanoma patient survival, and through additional functional enrichment analyses, we determined that these survival-related DEGs are largely related to inflammatory and immune responses. A prognostic signature comprised of 10 genes (*IL15*, *CCL8*, *CLIC2*, *SAMD9L*, *TLR2*, *HLA.DQB1*, *IGHV1-18*, *RARRES3*, *GBP4*, *APOBEC3G*) was generated. This 10-gene signature effectively separated melanoma patients into low- and high-risk groups based upon their survival. These low- and high-risk groups also exhibited distinct immune statuses and differing degrees of immune cell infiltration. In conclusion, our results offer novel insights into a number of microenvironment-associated genes that impact survival outcomes in melanoma patients, potentially highlighting these genes as viable therapeutic targets.

Abbreviations: AJCC = American Joint Committee on Cancer, AUC = area under the curve, DEGs = differentially expressed genes, ESTIMATE = estimation of Stromal and Immune cells in Malignant Tumor tissues using Expression data, FDR = false discovery rate, GSEA = gene set enrichment analysis, HR = hazard ratio, IFN = interferon, IL = interleukin, KEGG = Kyoto Encyclopedia of Genes and Genomes, LASSO = least absolute shrinkage and selection operator, OS = overall survival, PCA = principal component analysis, TCGA = The Cancer Genome Atlas, TME = tumor microenvironment.

Keywords: ESTIMATE, skin melanoma, TCGA

1. Introduction

Skin melanoma remains a highly malignant melanoma subtype, and it is also highly prevalent, accounting for approximately 4.6% of all malignant tumor types and 1.7% of cancer-related

death.^[1] Melanoma incidence has been rising in recent years, and although early state melanoma can readily undergo curative resection, the disease is often not detected until a later stage at which point the prognosis is poor. Indeed, advanced melanomas are often not responsive to chemotherapy or radiotherapy. However, as these tumors are often responsive to immunotherapeutic intervention, it is essential that novel immunomodulatory approaches to treating melanoma be developed.^[2]

Although tumor cells are often examined as individual entities, there is increasingly clear evidence that the local tumor microenvironment is essential for shaping tumor development.^[3,4] Microenvironmental cells and proteins can shape diverse tumor cell activities including survival and chemotaxis. This tumor microenvironment is also dynamic and is composed of stromal, immune, and endothelial progenitor cells, as well as a complex extracellular matrix and a diverse array of cytokines and growth factors.^[5] Immunological and stromal cells are the primary cells that drive melanoma growth and progression.^[6,7] Indeed, numerous immunomodulatory therapeutic approaches to treating melanoma have been designed in recent years.^[8,9] The ESTIMATE (Estimation of Stromal and Immune cells in Malignant Tumor tissues using Expression data) algorithm is a tool that is designed to gauge stromal and immune cell infiltration into a given tumor sample according to gene expression datasets.^[10] This algorithm has previously been used to evaluate microenvironmental composition associated with colon can-

Editor: Dan Lipsker.

The authors report no conflicts of interest.

Supplemental Digital Content is available for this article.

All data generated or analyzed during this study are included in this published article [and its supplementary information files].

Dermatological Department, Baoji Central Hospital, Shanxi, China.

* Correspondence: Wang Xiaoyuan, Dermatological department, Baoji Central Hospital, Shanxi 710000, China (e-mail: wangxiaoyuansur@163.com).

Copyright © 2021 the Author(s). Published by Wolters Kluwer Health, Inc. This is an open access article distributed under the terms of the Creative Commons Attribution-Non Commercial License 4.0 (CCBY-NC), where it is permissible to download, share, remix, transform, and build upon the work provided it is properly cited. The work cannot be used commercially without permission from the journal.

How to cite this article: Yingjuan W, Li Z, Wei C, Xiaoyuan W. Identification of prognostic genes and construction of a novel gene signature in the skin melanoma based on the tumor microenvironment. *Medicine* 2021;100:21 (e26017).

Received: 22 May 2020 / Received in final form: 28 April 2021 / Accepted: 29 April 2021

<http://dx.doi.org/10.1097/MD.00000000000026017>

cer,^[11] prostate cancer,^[10] and glioblastoma.^[12,13] However, no comparable studies regarding stromal and immune cell infiltration in melanoma have been conducted to date.

In the present analysis, we therefore evaluated melanoma patient The Cancer Genome Atlas (TCGA) genome expression profiles and the ESTIMATE algorithm to define the immune/stromal scores for these patients, leading us to identify a subset of microenvironment-associated genes related to melanoma patient overall survival (OS), then used these genes to construct a gene signature related to patient survival outcomes, and to explore the significance of this signature in relative to the immune response and immune cell infiltration. Together, our results offer novel insight into the melanoma tumor microenvironment while highlighting potential prognostically and/or therapeutically relevant gene targets in these tumors.

2. Materials and methods

2.1. Sample datasets

The raw mRNA expression data and clinical data of skin melanoma were downloaded from TCGA database (<https://gdc.nci.nih.gov/>). Extracted data were from patients with skin melanoma. In total, 470 skin melanoma samples (combined set) were divided into equally sized training and validation sets at random. The validation set was utilized when validating training set findings. As all data included herein were isolated from public sources, no ethical oversight was required.

2.2. DEG identification based on immune/stromal scores

ESTIMATE algorithm was applied to estimate the sample stromal and immune scores. Stromal and immune scores were calculated by the ESTIMATE package in R. ESTIMATE outputs stromal, immune and ESTIMATE scores by performing single-sample gene set enrichment analysis (GSEA). Based on immune/stromal score values, patients were divided into low- and high-score groups by median split. The expression profiles of melanoma patients with a high immune (or stromal) score were compared to those with a low score to identify immune (or stromal) score-related DEGs. The edge R package was then used for data analysis, with differentially expressed genes being defined as genes meeting the following criteria: false discovery rate (FDR) <0.05 and $|\log_2 \text{fold change}| > 1$.

2.3. Identification and functional enrichment analysis of survival-related DEGs

Univariate Cox regression analyses were used for identifying DEGs linked with melanoma patient survival using the 'survival' R package (bioconductor.org/packages/survival/). Prognostic DEGs were those with a log-rank $P < .05$. Functional enrichment analyses were used to identify potential pathways in which these survival-related DEGs were enriched. Kyoto Encyclopedia of Genes and Genomes (KEGG) pathway enrichment was assessed at a $P < .05$ significance threshold.

2.4. Development and validation of a survival-related DEG prognostic signature

A risk signature was constructed using these survival-related DEGs, with a least absolute shrinkage and selection operator (LASSO) regression strategy being employed to further screen

these genes and to optimize the risk signature. Prognostic risk score values were ultimately calculated as follows: Risk score = Gene 1 $\times \beta_1$ + Gene 2 $\times \beta_2$ + . . . Gene n $\times \beta_n$. The β symbol corresponds to a regression coefficient which had been defined for each gene of interest based upon the training dataset. Median prognostic risk score values were then employed for separating melanoma patients into low- and high-risk groups. This formula was then employed for assessing validation cohort patient samples. Signature prognostic relevance was gauged through univariate analyses of patients in both cohorts, after which the independent prognostic relevance of this signature risk score in these 2 cohorts was evaluated via multivariate analysis.

2.5. Bioinformatics analysis

We carried out a principal component analysis (PCA) to assess expression patterns for groups of patients, and GSEA was performed as a means of assessing whether there were significant differences between groups with respect to identified gene sets. We examined 2 gene sets (immune system process, M13664 and immune response, M19817) that were extracted from the Molecular Signatures Database v4.0 (<http://www.broadinstitute.org/gsea/msigdb/index.jsp>). We also examined KEGG gene sets from MSigDB. A normalized enrichment score <0.05 and FDR <0.05 were used to establish significance.

2.6. Immune infiltration analysis

The CIBERSORT algorithm^[14] was employed to transform skin melanoma gene expression profiles into the proportion of

Table 1
Clinical characteristics of combined, training, and validation cohort.

Characteristics	Combined cohort	Training cohort	Validation cohort
	n=470	n=235	n=235
Age, y	58.09 \pm 12.93	56.16 \pm 13.52	59.71 \pm 10.8
Sex			
Female	180 (38.29%)	93 (39.57%)	87 (37.02%)
Male	290 (61.71%)	142 (60.43%)	148 (62.98%)
T stage (8 th AJCC)			
T1	50 (10.64%)	25 (10.64%)	25 (10.64%)
T2	78 (16.59%)	30 (12.77%)	48 (20.43%)
T3	90 (19.15%)	44 (18.72%)	46 (19.57%)
T4	153 (32.55%)	78 (33.19%)	75 (31.91%)
Tx	99 (21.06%)	58 (24.68%)	41 (17.45%)
N stage (8 th AJCC)			
N0	235 (50%)	113 (48.09%)	122 (51.91%)
N1	74 (15.74%)	38 (16.17%)	36 (15.32%)
N2	49 (10.43%)	27 (11.49%)	22 (9.36%)
N3	55 (11.7%)	27 (11.49%)	28 (11.91%)
Nx	57 (12.13%)	30 (12.77%)	27 (11.49%)
M stage (8 th AJCC)			
M0	418 (88.94%)	198 (84.26%)	220 (93.62%)
M1	24 (5.11%)	18 (7.66%)	6 (2.55%)
Mx	28 (5.95%)	19 (8.08%)	9 (3.83%)
TNM stage (8 th AJCC)			
Stage I	89 (18.94%)	37 (15.74%)	52 (22.13%)
Stage II	140 (29.79%)	70 (29.79%)	70 (29.79%)
Stage III	171 (36.38%)	85 (36.17%)	86 (36.59%)
Stage IV	23 (4.89%)	17 (7.23%)	6 (2.55%)
Other	47 (10%)	26 (11.06%)	21 (8.94%)

AJCC = American Joint Committee on Cancer.

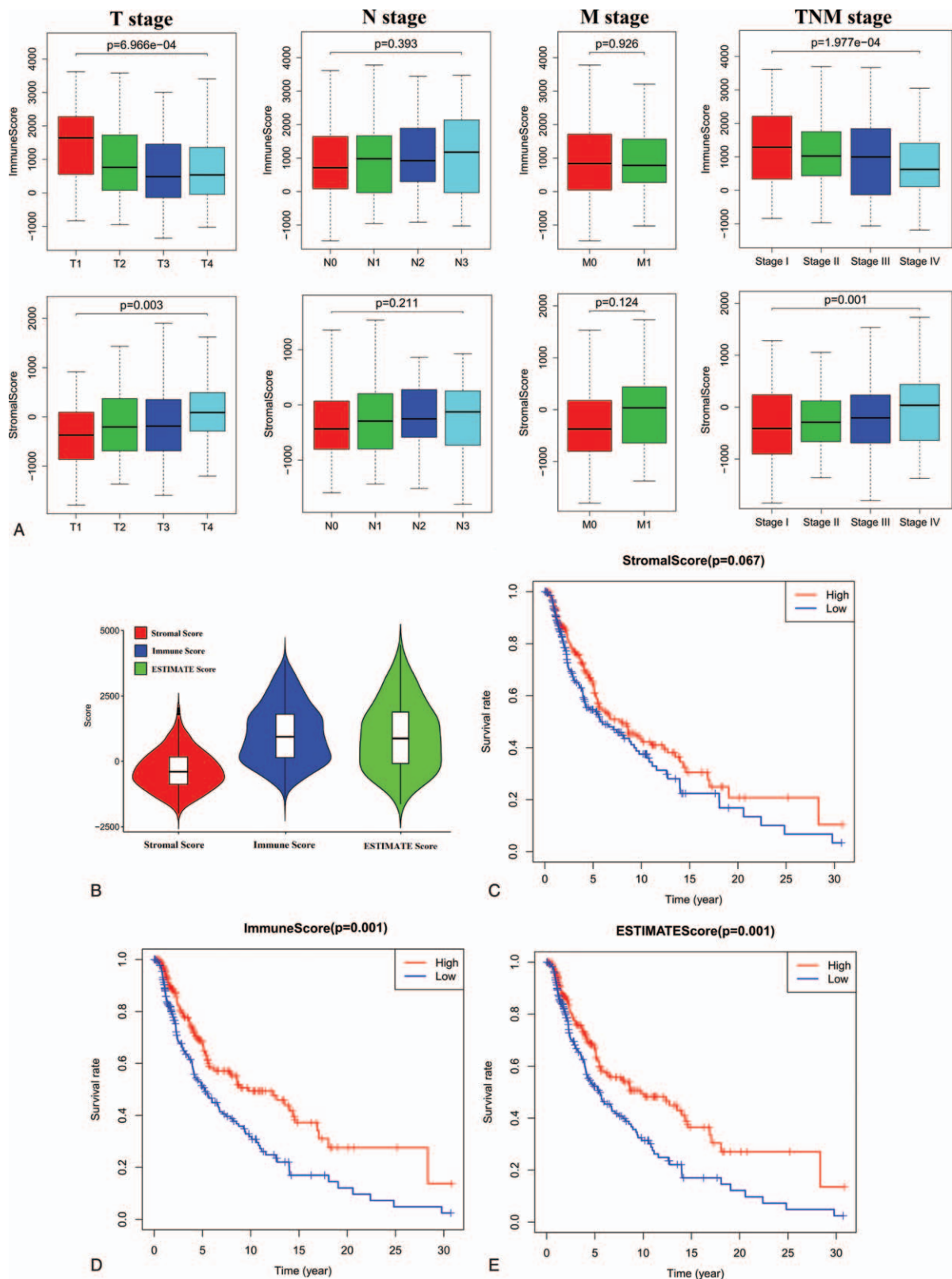


Figure 1. Association of stromal and immune scores with skin melanoma pathology and prognosis. (A) Distributions and comparisons of stromal and immune scores among different T stages, N stages, M stages, and TNM stages. (B) Violin plot of the stromal, immune and ESTIMATES scores. (C) Kaplan-Meier plot of overall survival for patients with low vs. high stromal scores. (D) Kaplan-Meier plot of overall survival for patients with low versus high immune scores. (E) Kaplan-Meier plot of overall survival for patients with simultaneously low ESTIMATES scores versus patients with high ESTIMATES scores.

22 tumor-infiltrating immune cells. The proportions of the 22 tumor-infiltrating immune cells in each sample were determined by using the “CIBERSORT” (R package). Features were compared between groups via 1-tailed *t* tests.

2.7. Statistical analysis

R (v3.6.3; <http://www.Rproject.org>) was employed for all analyses, with LASSO regression analyses being conducted using the “glmnet” package. The final gene signature was defined according to the sum of individual gene expression levels following weighting based upon gene-specific regression coefficients (β) values. Kaplan-Meier curves and log-rank tests were employed when conducting prognostic assessments, and figures were prepared with GraphPad Prism 8 (GraphPad Software Inc., CA). Univariate and multivariate Cox regression analyses were performed to identify predictors of patient prognosis. We utilized the “survival ROC” package for time-dependent receiver-operating characteristic curve analyses. $P < .05$ was the threshold of significance.

3. Results

3.1. Association of clinical characteristics with stromal/immune scores

We began by downloading TCGA gene expression data from 470 patients with skin melanoma (Table 1), including 290 males and

180 females (61.71% and 38.29%). The median age was 58.09 years (range: 15–90). Patients presented with AJCC 8th stage I, II, III, and IV tumors in 18.94%, 29.79%, 36.38%, and 4.89% of cases.

The ESTIMATE algorithm was then employed as a means of calculating stromal scores (range: –1800.51 to 1901.99), immune scores (range: –1476.28 to 3780.29) and ESTIMATE scores (range: –2618.28 to 5098.14) (Fig. 1 and Supplemental Table 1, <http://links.lww.com/MD/G120>). The link between stromal/immune scores and the pathologic properties of melanoma patients was evaluated by assessing score distributions among different T stages, N stages, M stages, and TNM stages. We found that these stromal/immune scores were significantly linked to T stage and TNM stage. Interestingly, stromal scores increased with increasing T stage ($P < .001$) and TNM stage ($P < .001$), whereas immune scores decreased with increasing T stage ($P < .001$) and TNM stage ($P < .001$). However, both stromal and immune scores were not significantly linked with N or M stage (all $P > .05$) (Fig. 1).

To explore the prognostic relevance of these immune and stromal scores, we separated patients into low- and high-score groups by median split (median stromal score = –330.28; median immune score = 862.96; median ESTIMATE score = 563.81). Subsequent Kaplan-Meier analyses revealed that patients with high immune and ESTIMATE scores exhibited an increase in OS relative to those for whom these scores were low ($P < .0001$) (Fig. 1).

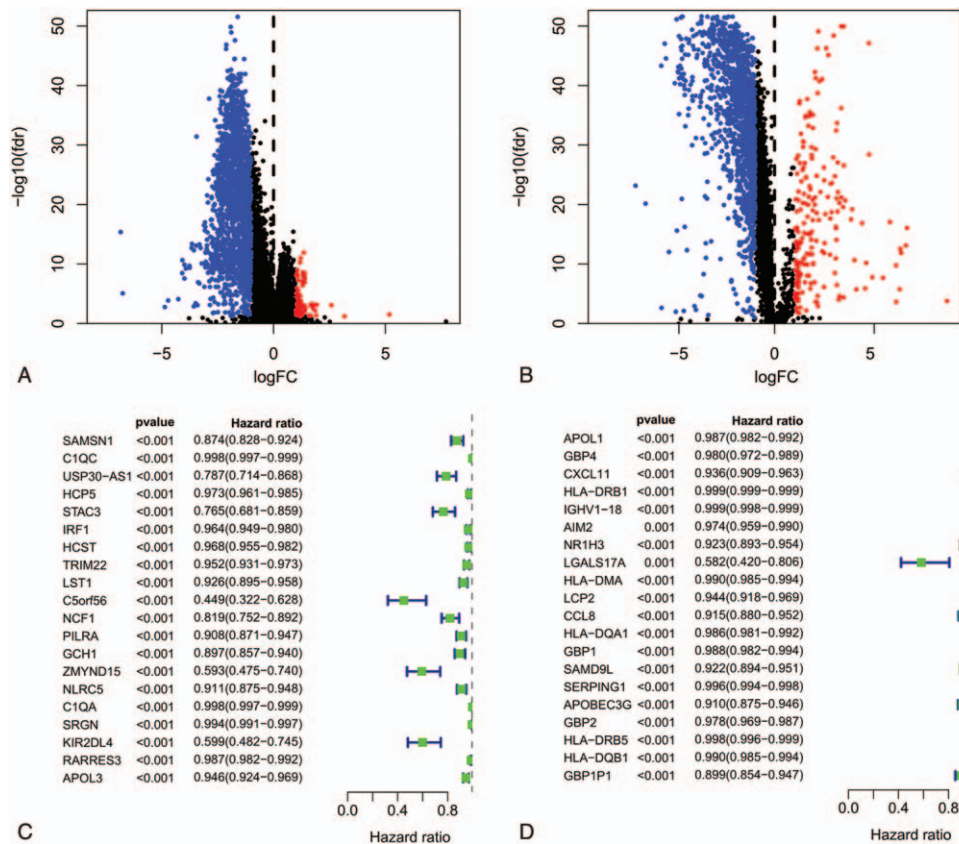


Figure 2. Volcano plot of differentially expressed genes (DEGs) from the low vs. high stromal score (A) /immune score (B) groups. Genes with $P < .05$ are shown in red (\log_2 fold change > 1.0) and blue (\log_2 fold change < -1.0). Black plots represent the remaining genes (those with no significant difference). Forest plot of hazard ratios for the top 20 stromal score(C)- and immune score(D)-related prognostic DEGs (hazard ratios and corresponding 95% confidence intervals were estimated by using the Cox proportional hazard regression model).

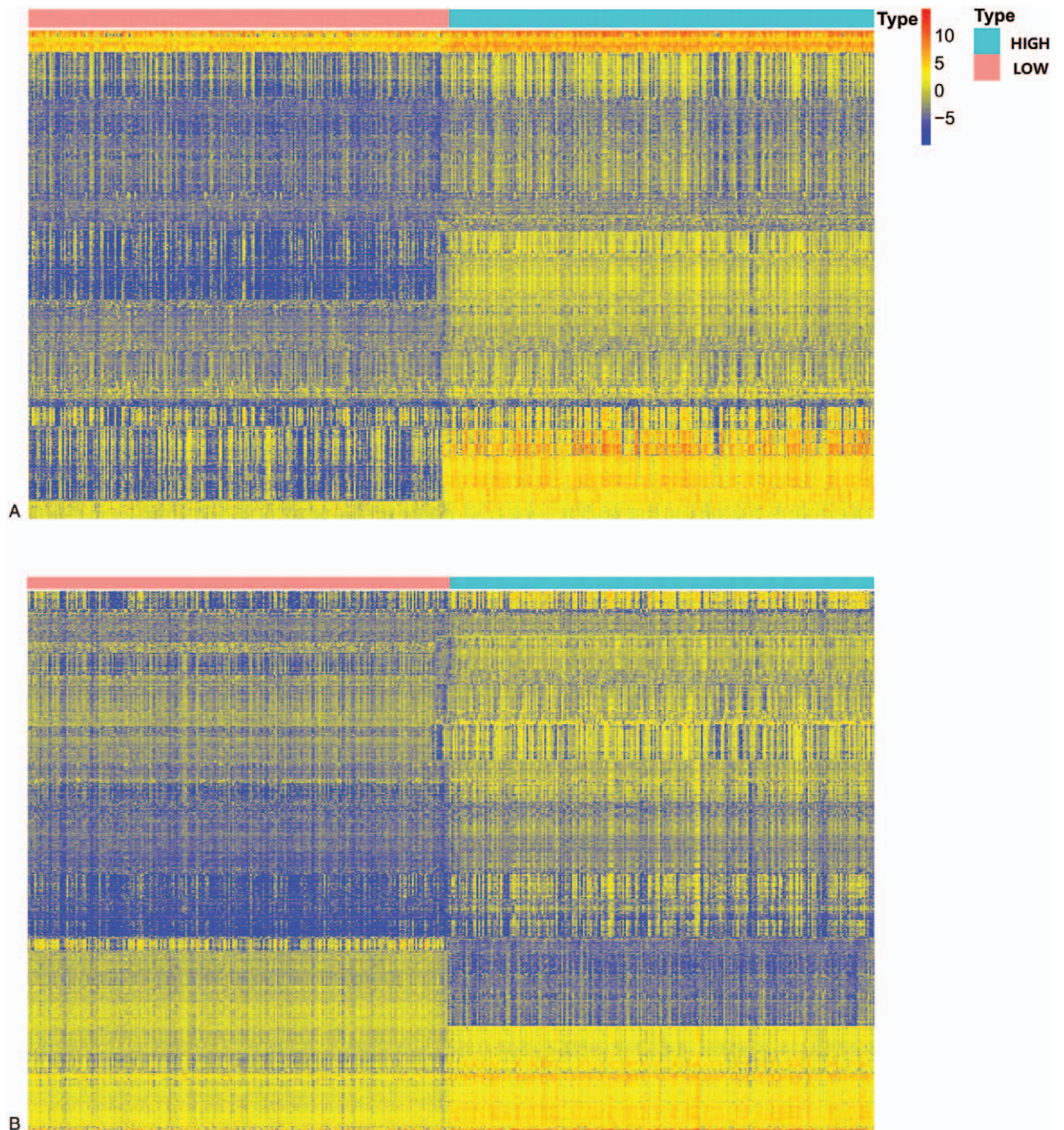


Figure 3. Expression profiles of stromal and immune score-related differentially expressed genes (DEGs). Heatmaps showing expression profiles for stromal score (A)- and immune score (B)-related DEGs with unsupervised hierarchical clustering analyses. Rows represent the DEGs expression profiles, and columns indicate corresponding tumor samples.

3.2. Identification of DEGs based upon immune/stromal scores

We assessed RNA-seq data from these 470 melanoma patients in the TCGA database in an effort to explore how gene expression levels and the immune/stromal scores generated above were related. The expression profiles of melanoma patients with a high immune (or stromal) score were compared to those with a low

score to identify immune (or stromal) score-related DEGs. In total, we identified 2054 stromal score-related DEGs (upregulated, $n = 1956$; downregulated, $n = 98$) and 1837 immune score-related DEGs (upregulated, $n = 1687$; downregulated, $n = 150$). ($FDR < 0.05$ and $|\log_2 \text{fold change}| > 1$) (Fig. 2 and Supplemental Table 2, <http://links.lww.com/MD/G121>). The expression profiles of stromal and immune score-related DEGs are visualized, respectively, on the heatmaps (Fig. 3).

3.3. Identification of the prognostic DEGs-based on OS

To determine the prognostic significance of these stromal/immune score-related DEGs in predicting melanoma patient OS, univariate Cox regression analyses were conducted to detect OS-associated DEGs. Among the 1837 immune score-related DEGs, 153 were significantly linked to melanoma patient OS. Using the same method, we identified 1006 stromal score-related DEGs that were significantly linked to melanoma patient OS (Fig. 2).

3.4. Functional enrichment analyses highlight the roles of survival-related DEGs

We next conducted KEGG functional enrichment analyses to assess these survival-related DEGs. KEGG analyses revealed that survival-

related DEGs (from immune score-related DEGs) were mainly enriched in neuroactive ligand-receptor interaction, cytokine-cytokine receptor interaction, JAK-STAT signaling, chemokine signaling, Th1 and Th2 cell differentiation, complement and coagulation cascades, and B cell receptor signaling pathways. Additionally, the survival-related DEGs (from stromal score-related DEGs) were primarily associated with antigen processing and presentation, cell adhesion molecules, the intestinal immune network for IgA production, and type I diabetes mellitus (Fig. 4).

3.5. Construction of a prognostic signature based on survival-related DEGs

Based on melanoma patient survival data in the training cohort, we used above survival-related DEGs as candidates for the

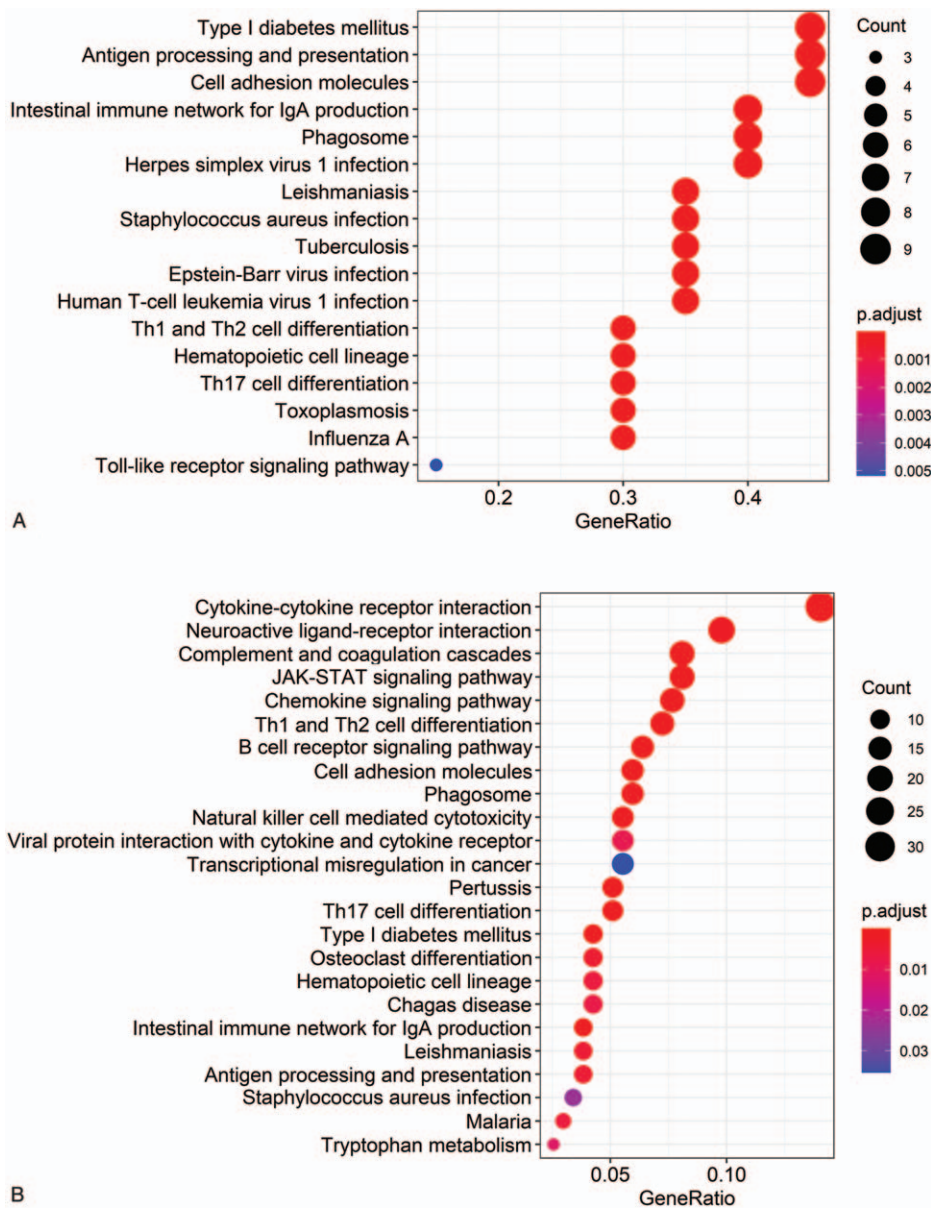


Figure 4. Kyoto Encyclopedia of Genes and Genomes (KEGG) pathway enrichment analysis of stromal score-related (A) and immune score-related (B) prognostic differentially expressed genes (DEGs). (x axis: the number of prognostic DEGs in each pathway; y axis: statistically Enriched KEGG pathway, P values were adjusted by false discovery rate).

Table 2
10-Gene signature.

Gene symbol	Gene ID	Description	Coefficient
<i>IL15</i>	80328	Interleukin 15	-0.03884
<i>CCL8</i>	6355	Chemokine (C-C motif) ligand 8	-0.00036
<i>CLIC2</i>	1193	Chloride intracellular channel protein 2	-0.00245
<i>SAMD9L</i>	219285	Sterile alpha motif domain containing 9-like	-0.00833
<i>TLR2</i>	7097	Toll-like receptor 2	-0.01267
<i>HLA.DQB1</i>	3119	Human leukocyte antigen DQB1	-0.00028
<i>IGHV1-18</i>	9606	Immunoglobulin heavy variable 1-18	-0.00014
<i>GBP4</i>	115361	GTP-binding protein 4	-0.00268
<i>RARRES3</i>	5920	Retinoic acid receptor responder (tazarotene induced) 3	-0.0013
<i>APOBEC3G</i>	60489	Apolipoprotein B mRNA editing enzyme, catalytic polypeptide-like 3G	-0.00163

construction of a gene risk signature. A LASSO Cox regression approach was employed to ultimately select 10 genes for inclusion in this signature (Table 2). We established a risk-scoring model based on the expression of 10-gene signature to predict survival. The risk score formula is as follows: risk score = $(-0.03884) \times \text{expr IL15} + (-0.00036) \times \text{expr CCL8} + (-0.00245) \times \text{expr CLIC2} + (-0.00833) \times \text{expr SAMD9L} + (-0.01267) \times \text{expr TLR2} + (-0.00028) \times \text{expr HLA.DQB1} + (-0.00014) \times \text{expr IGHV1-18} + (-0.00268) \times \text{expr GBP4} + (-0.0013) \times \text{expr RARRES3} + (-0.00163) \times \text{expr APOBEC3G}$. “expr” represents the expression value of the corresponding gene. To confirm the prognostic significance of the risk score. The median risk score (0.863) was identified as cutoff value to divide the patients into high- and low-risk group (Fig. 5).

Consistent with our expectations, low-risk melanoma patients (risk score ≤ 0.863) exhibited markedly increased OS compared to high-risk melanoma patients (risk score > 0.863) (16.39 ± 1.66 vs 6.37 ± 0.71 years, $P < .0001$). We then attempted to validate our signature-derived risk score by using this same approach to analyze the validation dataset, wherein we also found that the OS of low-risk patients was shorter than that of high-risk patients (11.71 ± 1.18 vs 7.24 ± 1.01 years; $P < .0001$). To compare the prognostic values of our 10-gene signature risk model and other clinicopathologic characteristics, we performed time-dependent receiver-operating characteristic curve analysis and the area under the curve (AUC) was measured. The 10-gene signature curve showed the greatest AUC value (training set: AUC=0.83; validation set: AUC=0.79) compared with other clinicopathologic characteristics curves in the training and the validation cohort. Thus, this 10-gene signature risk score may be more accurate than other clinical characteristics as a means of discriminating between melanoma patients (Fig. 6).

Independent risk factors in these two cohorts were assessed via univariate and multivariate Cox regression analyses. In univariate analyses, our 10-gene signature scores were significantly related with melanoma patient OS in the training (hazard ratio [HR]=199.59, 95% confidence interval [CI] 20.87–1908.94, $P < .001$) and validation (HR=38.93, 95% CI 6.45–234.94, $P < .001$) cohorts. Several clinicopathologic factors and the 10-gene signature scores were included in a multivariate analysis. These findings showed that 3 factors, including T stage (training set: HR=1.532, 95% CI 1.223–1.916, $P < .001$; validation set: HR=1.636, 95% CI 1.267–2.111, $P < .001$), N stage (Training set: HR=1.752, 95% CI 1.383–2.251, $P < .001$; validation set: HR=1.496, 95% CI 1.113–2.01, $P = .008$), and the 10-gene signature score (training set: HR=42.11, 95% CI 8.243–

216.463, $P < .001$; validation set: HR=13.54, 95% CI 1.91–96.19, $P = .009$) were independent prognostic indicators in the training and validation cohorts (Table 3).

3.6. High- and low-risk melanoma patients exhibit differences in immune status and infiltration

A PCA approach was employed to evaluate differences in patterns of distribution in the low- and high-risk groups based upon 10-gene signature risk scores, and the low- and high-risk groups were separable into 3 distinct clusters (Fig. 7). A GSEA functional annotation strategy was also employed, revealing low-risk samples to be significantly enriched for immune response pathway-related genes compared to those from high-risk patients. There were therefore clear differences in the immune status of tumor samples from low- and high-risk melanoma patients when these patients were stratified according to their 10-gene signature risk scores. Furthermore, low-risk group samples were enriched for immunological pathways such as the JAK-STAT, RIG-I-like receptor, Toll-like receptor, and T cell receptor signaling pathways. However, the enriched pathways in the high-risk group were predominantly associated with oxidative phosphorylation, glyoxylate metabolism, and dicarboxylate metabolism (Fig. 7).

We next performed an immune cell-based analysis, revealing low-risk patients to have increases in numbers of M1 macrophages, naïve/memory B cell, plasma cells, regulatory T cells (Tregs), CD8+ T cells, activated CD4+ memory T cells, follicular helper T cells, and resting NK cells. In contrast, high-risk patients had increases in M2 macrophage and M0 macrophage levels. Our 10-gene signature risk scores were also negatively correlated with enrichment for B cell, CD4+ T cells, CD8+ T cells, dendritic cells, neutrophils, and macrophages (Fig. 8).

4. Discussion

Melanomas are not homogenous, but comprise cells with differing invasive, proliferative and stem-like phenotypes. Accumulating evidence suggests that the proliferative and invasive cells in melanoma are characterized by distinct gene expression profiles. Notably, the tumor microenvironment (TME) can induce melanoma cells to alternate between these phenotypes.^[15] Previous work suggests that both immune and stromal cells represent key facets of the TME, and can profoundly impact tumor proliferation, progression, and therapeutic responsiveness.^[16] As such, it is essential that further studies evaluate the

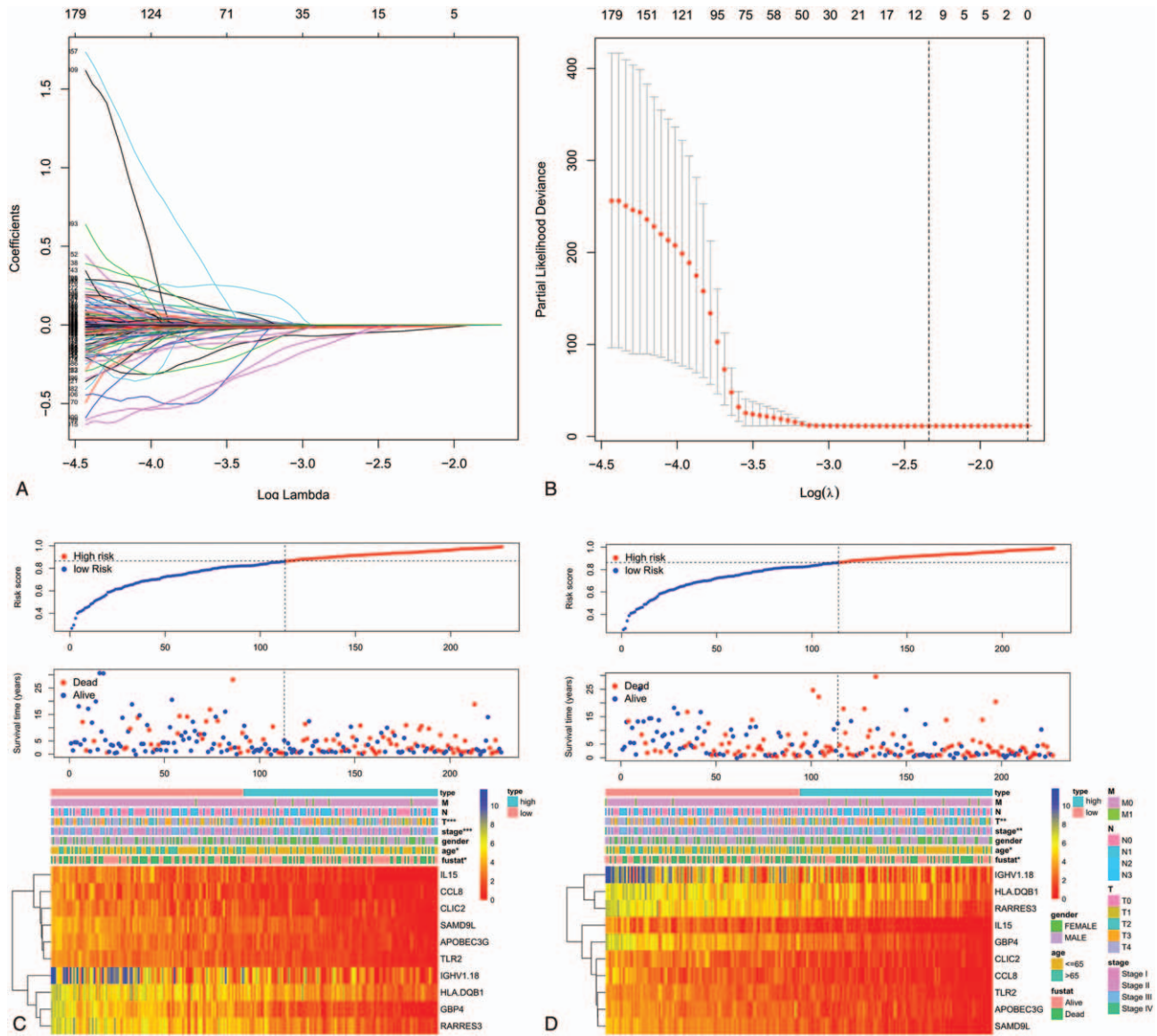


Figure 5. Construction and validation of 10-gene signature risk score model. (A) LASSO coefficient spectrum of 10 genes in skin melanoma. Generate a coefficient distribution map for a logarithmic (λ) sequence. (B) Selecting the best parameters for skin melanoma in the LASSO model (λ). Distribution of risk score, OS, gene expression, and clinicopathologic features in in the training (C) and validation (D) datasets. Heatmap of the expression of 10 microenvironment-related prognostic genes in low-risk and high-risk groups (Rows represent corresponding genes, whereas columns indicate corresponding patients). Clinicopathologic features in low-risk and high-risk groups stratified by the signature. Rows represent corresponding items (T stage, N stage, M stage, TNM stage, age, and sex). Cases in low-risk group displayed lower age, T and TNM stage in training and validation. ($P < .05$, $**P < .01$, $***P < .001$).

genomic profiles associated with extant tumor sequencing datasets to better evaluate the interplay between melanoma cells and the TME. Herein, we therefore evaluated the prognostic relevance of TME-related genes within the TCGA dataset. Initially, we utilized the ESTIMATE algorithm to establish stromal and immune cell scores for melanoma patients. We then determined that melanoma patients with higher immune scores exhibited significantly improved OS relative to patients with low immune scores. We identified DEGs associated with the immune/stromal scores generated for these patient samples, and we then utilized patient outcome data in order to identify survival-related DEGs. These genes were incorporated into a prognostic risk signature that was used to compare differences in OS and

immune cell infiltration between low- and high-risk melanoma patients.

We additionally conducted functional enrichment analyses of survival-related DEGs suggesting that these genes were associated with cytokine-cytokine receptor interactions, complement and coagulation cascades, JAK-STAT signaling, chemokine signaling, Th1 and Th2 cell differentiation, and B cell receptor signaling pathways. Together, these results suggest that these survival-related DEGs are largely associated with immune and inflammatory responses. The immune microenvironment has previously been shown to profoundly shape melanoma progression and prognosis, and there have been many efforts to date to develop novel immunotherapeutic approach.

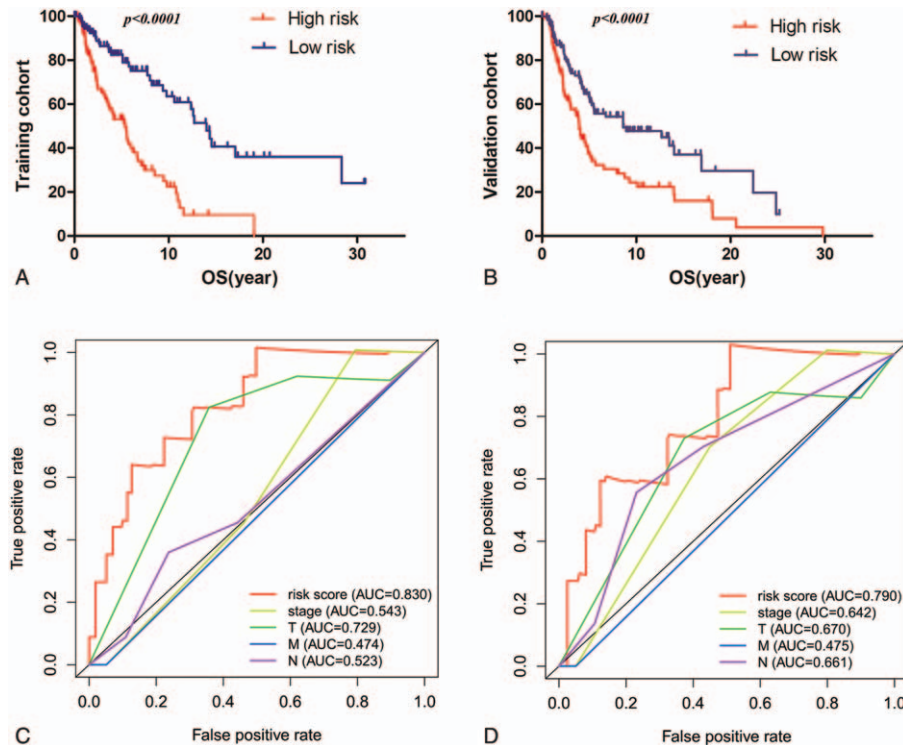


Figure 6. Kaplan-Meier analysis of patients' OS in the high-risk and low-risk subgroups of the training cohort (A) and validation cohort (B). The x axis represents the survival time (years), and the y axis represents survival rate; time-dependent ROC analysis performed to compare the ten-gene signature risk model and other clinicopathologic characteristics in predicting OS of skin melanoma in training cohort (C) and validation cohort (D). OS = overall survival.

Herein, we incorporated a subset of these survival-related DEGs into a gene signature risk model. Risk scores derived from this model were then employed as a means of separating patients into low- and high-risk groups, with subsequent analyses confirming that there were significant differences in patient OS between these 2 risk cohorts that corresponded to a high AUC value. We

additionally confirmed the independent prognostic relevance of this risk score in melanoma patient samples through univariate and multivariate analyses. Together, these results offer novel insight into the role of the TME as a regulator of melanoma. A subset of the 10 genes included in our risk signature has previously been studied in the context of melanoma, including interleukin (IL)-15 which is

Table 3

Univariate and multivariate independent prognostic analysis of 10-gene signature risk score and other clinical characteristics in melanoma patients.

Characteristic	Univariate analysis		Multivariate analysis	
	HR (95% CI)	P	HR (95% CI)	P
Training cohort				
Age	1.024 (1.004–1.037)	<.001	1.011 (0.997–1.024)	.087
Gender	0.958 (0.665–1.368)	.788	0.892 (0.685–1.423)	.891
T stage	1.575 (1.321–1.978)	<.001	1.532 (1.223–1.916)	<.001
N stage	1.589 (1.352–1.905)	<.001	1.752 (1.383–2.251)	<.001
M stage	1.557 (0.576–4.173)	.387	1.591 (0.521–4.812)	.408
TNM stage	1.568 (1.287–1.912)	<.001	0.767 (0.519–1.129)	.177
Signature risk score	199.59 (20.87–1908.94)	<.001	42.11 (8.243–216.463)	<.001
Validation cohort				
Age	1.025 (1.010–1.039)	<.001	1.005 (0.989–1.021)	.547
Sex	1.182 (0.766–1.822)	.451	0.879 (0.556–1.391)	.583
T stage	1.776 (1.437–2.195)	<.001	1.636 (1.267–2.111)	<.001
N stage	1.425 (1.164–1.746)	<.001	1.496 (1.113–2.01)	.008
M stage	3.466 (0.84–14.295)	.086	1.253 (0.283–5.555)	.767
TNM stage	1.607 (1.255–2.058)	<.001	0.978 (0.631–1.516)	.922
Signature risk score	38.93 (6.45–234.94)	<.001	13.54 (1.91–96.19)	.009

HR = hazard ratio.

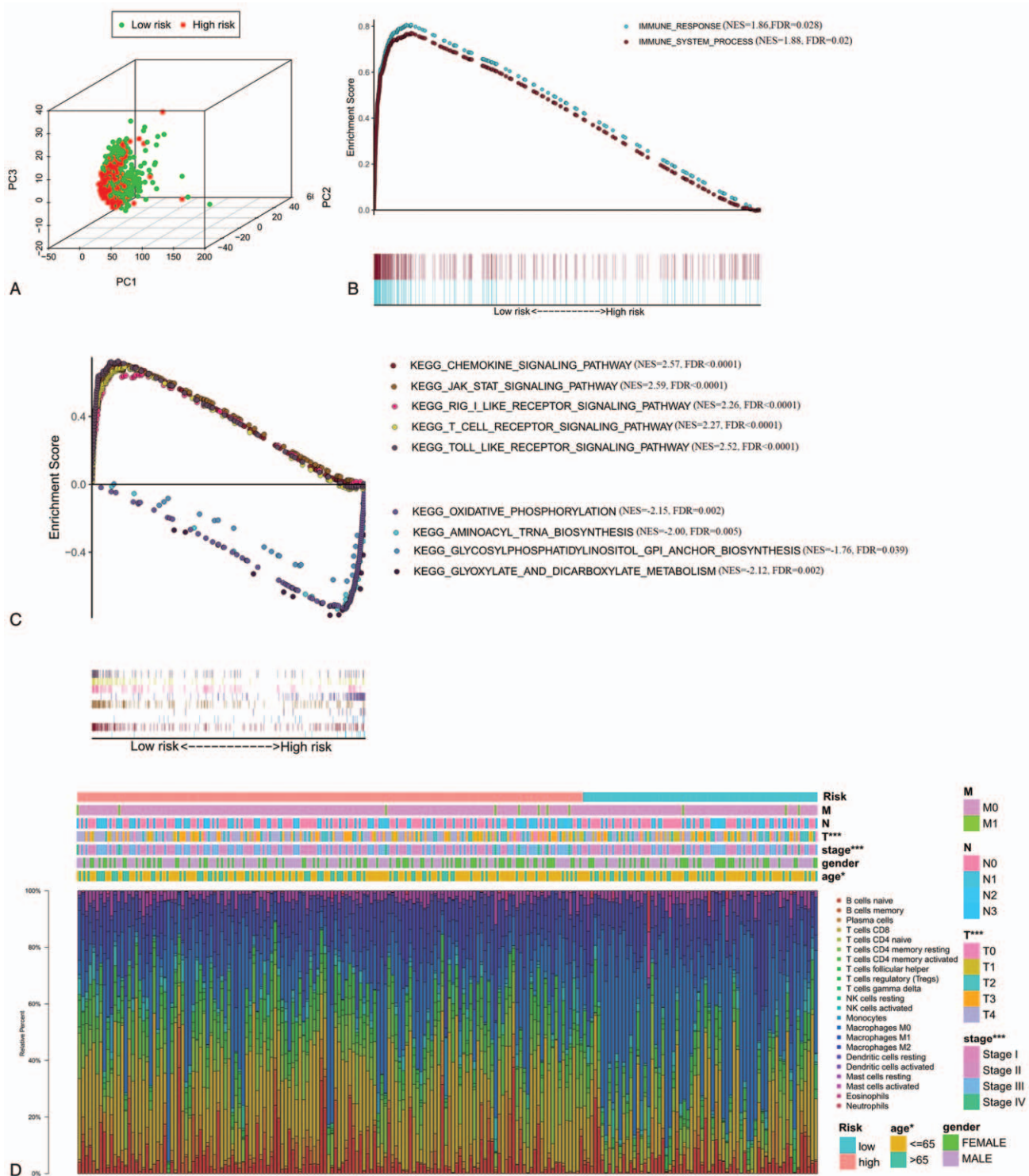


Figure 7. (A) Principal components analysis between low- and high-risk groups on the basis of the 10-gene signature risk score model. Functional annotation of the 10-gene signature by GSEA analysis: (B) Immune response set and Immune system process set (C) Kyoto Encyclopedia of Genes and Genomes. (D) Microenvironment of the immune cell population is estimated by CIBERSORT algorithm based on TCGA-skin melanoma data (Row: tumor samples). Clinicopathologic features in low-risk and high-risk groups (corresponding items: T stage, N stage, M stage, TNM stage, age, and sex. * $P < .05$, ** $P < .01$, *** $P < .001$). FDR = false discovery rate, NES = normalized enrichment score.

a multifunctional cytokine related to NK, T, and B cell survival and activation. The ability of IL-15 to suppress tumor progression and metastasis in animal melanoma model systems (including B16 and B78-H1 tumor models) has previously been demonstrated and

linked to its ability to facilitate CD8+ T cell and NK cell activation and proliferation.^[17]

High- and low-risk groups were also significantly different with respect to observed immune cell infiltration. TME composition is

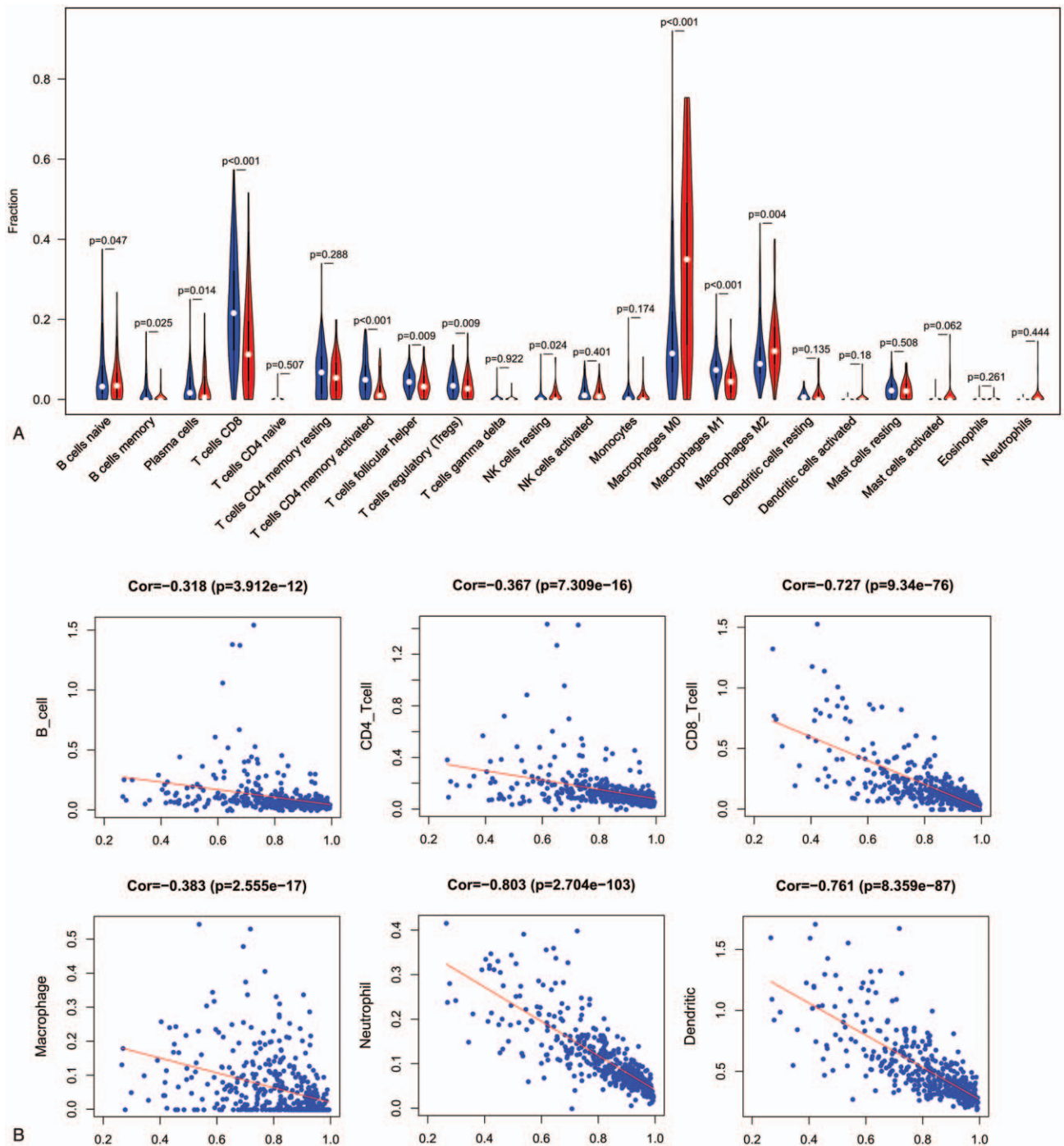


Figure 8. (A) The violin plot showed the immune cells population in the low- (blue) and high-risk (red) groups. *P* values are based on the Wilcoxon Test. (B) Correlation analysis between immune cells population and risk score. *P* values are based on the paired *t* test.

of significant research interest. The immune cells within the melanoma tumor microenvironment, however, can vary widely and is associated with patient prognosis. Tumor-infiltrating lymphocytes—in particular CD8+ T cells—serve as key mediators of tumor immune surveillance.^[18–20] Normally, effector CD8+ T cells are activated upon antigen and costimulatory molecule exposure, whereupon they can lyse tumor cells and suppress the growth of tumors. Itay et al^[21] confirmed the distinct exhaustion status of CD8+ T cells in melanoma

patients and defined a core exhaustion-gene signature through the single-cell RNA-seq. The exhaustion of CD8+ T cells have been shown to be important regulators of melanoma patient prognosis. In line with these results, we found that high-risk melanoma patients in our patient sample cohort exhibited decreased CD8+ T cell infiltration relative to low-risk patients. Tregs are another cell type of prognostic interest that are commonly evaluated, although their relevance in the context of melanoma remains uncertain. Many studies have shown Treg

infiltration to be associated with a poorer melanoma patient prognosis, although there are some reports suggesting that they have a neutral or negligible impact on patient outcomes. Shang et al.^[22] found that FoxP3⁺ Tregs were of greater prognostic relevance in COX-2⁺ melanoma patients than in those with COX-2⁻ disease in a meta-analysis. Herein, however, we found Tregs to be enriched in low-risk patients. B cells, however, are not known to be as important as T cells in this setting, with inconsistent prognoses having been identified as a function of B cell status such that the importance of B cells remains uncertain. Herein, we demonstrated a significant negative correlation between B cells and risk score, and naive B/plasma cells were enriched in low-risk patients. However, the exact impact of these findings on patient prognosis remains to be established.

Tumor-associated macrophages are also key regulators of the interactions between tumor cells and the immune system. Traditionally, tumor-associated macrophages are classified as being polarized towards an M1 or an M2 phenotype. M2 macrophage infiltration within tumors has been linked to a poorer patient prognosis owing to the anti-inflammatory, angiogenic, and extracellular matrix remodeling activities of these cells. We found M2 macrophages to be enriched in samples from high-risk melanoma patients. However, we have limited knowledge of how to achieve a balance between M1- and M2-phenotypes. JAK/STAT signaling pathways are among the most important regulators of polarization. GSEA results revealed that signaling pathways including JAK/STAT signaling pathways were enriched in low-risk group. Interferon (IFN)- γ can induce M1 macrophage polarization, and IFN- γ can activate STAT1, with the IFN- γ /JAK/STAT1 signaling pathway functioning as a key mechanism regulating the M1 phenotype. Previous work has shown that IL-6/JAK/STAT3 signaling pathway activation primarily mediates macrophage M2 polarization.

There are multiple limitations to the present study. For one, this analysis was retrospective in nature, and so future prospective studies will be essential to validate these results. In addition, functional analyses of the identified prognostic DEGs are essential before their clinical application to fully explore their roles in melanoma and their prognostic relevance. In addition, it is important to note that the immune signature identified in the present study is based upon an estimate of immune cell infiltration within tumors as determined from algorithmic analyses of RNA-seq data. Future in-depth research will be essential to confirm the validity of these immune infiltration results, and to assess the cell–cell interactions that may occur within these tumors and that may impact melanoma progression or prognosis.

5. Conclusion

Herein, we conducted a comprehensive bioinformatics analysis of TCGA melanoma patient gene expression datasets to evaluate the melanoma tumor microenvironment. Through this approach, we identified microenvironment-related DEGs and then evaluated their prognostic relevance in melanoma patients. Future clinical studies of the functional roles of these genes will be essential to fully validate their relationship to patient survival outcomes. Overall, our results offer new insight into the complex interplay between melanoma stromal cells and immune cells within the

tumor microenvironment, potentially highlighting novel therapeutic targets for future clinical evaluation.

Author contributions

Writing – original draft: Wang Yingjuan, Zhang Li, Cao Wei.

Writing – review & editing: Wang Xiaoyuan.

References

- Ahmedin J, Freddie B, Melissa MC, et al. Global cancer statistics [J]. *Ca Cancer J Clin* 2011;61:69–90.
- Boyle P, Ferlay J. Cancer incidence and mortality in Europe [J]. *Ann Oncol* 2005;16:481488.
- Reisfeld RA. The tumor microenvironment: a target for combination therapy of breast cancer[J]. *Crit Rev Oncogen* 2013;18:115–33.
- Yang L, Wang S, Zhang Q, et al. Clinical significance of the immune microenvironment in ovarian cancer patients [J]. *Mol Omics* 2018; 14:341–51.
- Ayala F, Dewar R, Kieran M, Kalluri R. Contribution of bone microenvironment to leukemogenesis and leukemia progression. *Leukemia* 2009;23:2233–41.
- Austin R, Smyth MJ, Lane SW. Harnessing the immune system in acute myeloid leukaemia. *Crit Rev Oncol Hematol* 2016;103:62–77.
- Yehudai-Resheff S, Attias-Turgeman S, Sabbah R. Abnormal morphological and functional nature of bone marrow stromal cells provides preferential support for survival of acute myeloid leukemia cells. *Int J Cancer* 2019;144:2279–89.
- Beyar-Katz O, Gill S. Novel approaches to acute myeloid leukemia immunotherapy. *Cancer Res* 2018;24:5502–15.
- Vandsemb EN, Kim TK, Zeidan AM. Will deeper characterization of the landscape of immune checkpoint molecules in acute myeloid leukemia bone marrow lead to improved therapeutic targeting? *Cancer* 2019; 125:1410–3.
- Yoshihara K, Shahmoradgoli M, Martinez E, et al. Inferring tumour purity and stromal and immune cell admixture from expression data. *Nat Commun* 2013;4:2612.
- Shah N, Wang P, Wongvipat J, et al. Regulation of the glucocorticoid receptor via a BET-dependent enhancer drives antiandrogen resistance in prostate cancer. *eLife* 2017;6:
- Alonso MH, Aussó S, Lopez-Doriga A, et al. Comprehensive analysis of copy number aberrations in microsatellite stable colon cancer in view of stromal component. *Br J Cancer* 2017;117:421–31.
- Jia D, Li S, Li D, et al. Mining TCGA database for genes of prognostic value in glioblastoma microenvironment. *Aging* 2018;10:592–605.
- Newman AM, Liu CL, Green MR, et al. Robust enumeration of cell subsets from tissue expression profiles. *Nat Methods* 2015;12:453–7.
- Ennen M, Keime C, Kobi D, et al. Single-cell gene expression signatures reveal melanoma cell heterogeneity[J]. *Oncogene* 2015;34:3251–63.
- Gregor S, Francesca F, Florent P, et al. Comprehensive evaluation of transcriptome-based celltype quantification methods for immunology. *Bioinformatics* 2019;35:i436–45.
- Dubsky P, Saito H, Liogier M, et al. IL-15-induced human DC efficiently prime melanoma-specific naive CD8⁺ T cells to differentiate into CTL[J]. *Eur J Immunol* 2007;37:1678–90.
- Edwards J, Wilmott JS, Madore J, et al. CD103⁺ tumor-resident CD8⁺ T cells are associated with improved survival in immunotherapy-naïve melanoma patients and expand significantly during Anti-PD-1 treatment [J]. *Clin Cancer Res* 2018;24: clincanres.2257.2017.
- Montinaro A, Forte G, Sorrentino R, et al. Adoptive immunotherapy with Cl-IB-MECA-treated CD8⁺ T cells reduces melanoma growth in mice [J]. *PLoS One* 2012;7:e45401.
- 2015;Kohlhapp FJ, Broucek JR, Hughes T, et al. NK cells and CD8⁺ T cells cooperate to improve therapeutic responses in melanoma treated with CTLA-4 blockade and IL-2 (TUM2P. 1039) [J]. 3:18.
- Tirosh I, Izar B, Sanjay PM, et al. Dissecting the multicellular ecosystem of metastatic melanoma by single-cell RNA-seq[J]. *Science* 2016; 352:189–96.
- Shang B, Liu Y, Jiang SJ, et al. Prognostic value of tumor-infiltrating FoxP3⁺ regulatory T cells in cancers: a systematic review and meta-analysis[J]. *Sci Rep* 2015;5:15179.